INCLINED MAGNETIC FIELD EFFECTS ON MARANGONI FLOW OF CARREAU LIQUID

Rahila NAZ [*1], Fazle MABOOD[2], Tasawar HAYAT[3,4]

[*1]Department of Applied Mathematics and Statistics, Institute of Space Technology, P.O.Box 2750 Islamabad 44000, Pakistan

[2]Department of Mathematics, University of Peshawar, P.O.Box 25120, Peshawar Pakistan

[3]Department of Mathematics, Quaid-i-Azam University, P.O.Box 45320, Islamabad 44000, Pakistan

[4]Department of Mathematics, Faculty of Science, King Abdulaziz University, P.O.Box 80257, Jeddah 21589, Saudi Arabia

[*]Corresponding author; E-mail: eyya1@hotmail.com

Marangoni convection flow of Carreau liquid by an inclined porous surface is addressed. Magnetic field is taken inclined. Nonlinear thermal radiation effects are incorporated considering the Rosseland's approximation. Runge-Kutta Fehlberg fourth fifth (RKF-45) order scheme is utilized to solve the nonlinear equations subject to nonlinear convective boundary conditions. Nonlinear expression of Nusselt number is derived. Concrete graphical description is present out for flow velocity, temperature and Nusselt number. Numerical treatment of nonlinear Nusselt number is performed and analyzed.

Key words*: Marangoni convection; Carreau liquid; inclined magnetic field, nonlinear thermal radiation; inclined surface; numerical solution.*

1. Introduction

Marangoni convection arise due to the surface tension gradient in the interfacial liquid flow. It accelerates the procedures of heat and mass transfer. Such consequence is employed in stabilizing the soap films, drying the silicon wafers in the manufacturing of integrated circuits, self-assembling of the nanoparticles into ordered arrays, semiconductor processing, welding, nucleation etc. Recently, Zhao et al. [1] carried out Marangoni convection effect in flow of Maxwell fluid. They adopted numerical procedure for the fractional flow model and studied the characteristics of surface tension and heat transfer performance in the flow field. Analysis of Marangoni effect for single-wall (SWCNTs) and multi-wall carbon nanotubes (MWCNTs) is carried out by Hayat et al. [2]. They found that multi-wall carbon nanotubes (MWCNTs) moves fast as compared to the single-wall carbon nanotubes (SWCNTs) and thermal radiation heats up the fluid. Sheikholeslami and Ganji [3] inspected the Marangoni convection effect for forced convection heat transfer of CuO-H_2O nanofluid. They developed the solution using Runge-Kutta integration method and investigated that the Lorentz force reduces the nanofluid's velocity. Discussion on Marangoni convection is made by Aly and Ebaid [4]. They worked on nanofluid with the effects of magnetic filed, thermal radiation, suction/injection and porous medium. They deliberate over the physical insight of the flow and observed that the effective electrical conductivity makes a very considerable and remarkable effect on the nanofluids' flow. Hayat et al. [5] developed the analytic solutions for the momentum and energy equations considering Marangoni convection of Casson fluid. They found the velocity to be an increasing function of mixed convection parameter for assisting flow whereas reverse impact is reported for the opposing flow. The The Carreau fluid model lies in the category of generalized Newtonian fluids whose viscosity depends upon the rate of shear. It reduces to the classical Newtonian model when the power law index is numerically equal to 1. This model also overcomes the shortcomings of the power-law model by describing the viscosity for very small / large shear rates. Carreau fluid is attracted by many researchers in literature. Khan et al. [6] examined the Carreau nanofluid flow in an expanding\contracting cylinder with heat and mass transfer processes. They considered the temperature dependent thermal conductivity and computed the numerical results through bvp4c scheme. They considered both the shear thinning and shear thickening cases. Carreau-Yasuda fluid for unsteady squeezed flow model has been considered by Salahuddin et al. [7]. They considered the flow through horizontal sensor surface and numerical solution has been computed by Runge-Kutta-Fehlberg scheme. Hashim and Masood [8] examined the Carreau fluid flow with Cattaneo-Christov heat transfer effects. They computed the numerical solutions through Runge-Kutta Fehlberg iterative scheme. They explained that the flow velocity and the temperature were decelerated for higher values of the wall thickness parameter. A peristaltic study of Carreau-Yasuda fluid in a curved conduit is conducted by Abbasi et al. [9]. Flow situation is described through lubrication approach and the properties of Hall effects are discussed in a curved conduit. Flow of Carreau-Yasuda fluid for Hall and MHD effects is examined by Hayat et al. [10]. They considered the curved walls and enlightened the processes of heat and mass transfer. Effectiveness of inclined magnetic field is considered by scientists and engineers for example its role for the stagnation point flow of nanofluid is given by Hayat et al. [11]. They evolved the solutions for momentum, energy and mass transfer equations considering the heat generation/absorption and thermal radiative processes in heat transfer. Khan et al. [12] assumed the oscillatory oblique stagnation point flow for the nanofluid with nanoparticles of Copper (Cu), Alumina (Al2O3) and Titania (TiO2). They calculated the graphical and tabular results for the flow configuration. Sivaraj and Sheremet [13] constructed the solution for viscous fluid flow in an inclined porous cavity with the effects of inclined uniform magnetic field. They established Brinkman-extended Darcy model and calculated the numerical solutions for different inclinations. An inclined channel is considered by Abbas et al. [14] for two phase flow of magnetite-water using inclined magneto convection, radiative heat transfer and slip effects. They developed a nonlinear differential model and computed the analytic solutions. Shahzadi and Nadeem [15] contributed their work for the nanofluid flow with an inclined magnetic field effects. The transfer of heat through radiation performs an important role for the engineering mechanisms at high temperatures. Radiative heat transfer also has significant importance in space technology for dealing with solar energy, in polymer industry for the extrusion of polymers, in nuclear industry for controlling the heat transfer mechanism and many engineering processes. Particularly, radiative heat transfer in electrically conducting fluids is more important for the nuclear and industrial engineering purposes for example the design of equipment, gas turbines and several propulsion devices for aircraft missiles, nuclear plants, space vehicles and satellites. The literature reveals that radiative heat transfer is discussed in many researches. Radiative heat transfer study of a Jeffrey viscoelastic fluid with dust-particle suspensions is carried out by Bhatti et al. [16]. They developed the electro-magneto-hydrodynamic peristaltic flow in planar channel containing a homogenous porous medium. They constructed the analytic solution and discussed the dusty fluid dynamics in detail through graphs and tables. Nonlinear thermal radiation effects for thin liquid film with heat source/sink and chemical reaction are discussed by Pal and Saha [17]. They developed the flow over an unsteady porous stretching surface considering the convective boundary conditions. They used the shooting method together with Runge-Kutta-Fehlberg technique and enlighten the significant parametric effects on velocity and temperature profiles. Hsiao [18] developed the forced and free convection stagnation point flows of an electrically conducting Maxwell fluid. Joule heating, nonlinear radiation, thermal conductivity and convective heat transfer are considered. Finite difference scheme is applied to get the solutions. Nonlinear Rosseland approximation is used for radiative heat transfer of two viscoelastic fluids by R. Cortell [19]. Das et al. [20] discussed the nonlinear radiative heat flux in flow of Jaffery fluid over a stretching sheet. They utilized the Runge-Kutta-Fehlberg scheme to compute the solutions.

The aforementioned studies depict that heat transfer through nonlinear thermal radiation is not much examined. Marangoni flows are also less attended for realistic fluids because of the highly nonlinear boundary conditions. Flows by an inclined channel with different inclination of magnetic field is also not discussed. Motivated by these facts, we study the Marangoni convective flow of an electrically conducting Carreau fluid over a porous inclined surface. Nonlinear thermal radiation, thermal conductivity, Joule heating and viscous dissipation effects are accounted. Runge-Kutta Fehlberg scheme [21-24] is utilized to compute the numerical solutions. The article is structured as follows. First section contributed toward the brief introduction of study. In second section, mathematical problem is formulated and nondimensionalized. Third section comprises the numerical procedure. Analysis and comparison of study with Hayat et al. [25] are given in fourth section whereas conclusions are presented in section five. References are listed in the sixth section.

2. Problem statement

In this paper the steady Marangoni convection flow driven by a temperature gradient in electrically-conducting Carreau liquid is considered. The two-dimensional analysis is presented by an inclined surface [5]. Effects of magnetohydrodynamics, buoyancy and external pressure gradient are considered. Permeable surface subject to suction / injection is taken. Analysis of heat transfer is carried out through viscous dissipation, Joule heating and thermal radiation. Thermal stratification is also considered. The governing equations of this study are based on the balance laws of mass, momentum and energy. Taking the above assumptions into consideration, the boundary layer equations can be written in dimensional form as:

$$\frac{\partial u}{\partial x}+\frac{\partial v}{\partial y}=0, \tag{1}$$

$$u\frac{\partial u}{\partial x}+v\frac{\partial u}{\partial y}=-\frac{\Delta B_0^2}{\rho}u\sin^2\psi+\nu\left[1+\lambda^2\left(\frac{n-1}{2}\right)\left(\frac{\partial u}{\partial y}\right)^2\right]\frac{\partial^2 u}{\partial y^2}$$
$$+\nu(n-1)\lambda^2\left[1+\lambda^2\frac{3}{4}\left(\frac{n-3}{2}\right)\left(\frac{\partial u}{\partial y}\right)^2\right]\frac{\partial^2 u}{\partial y^2}\left(\frac{\partial u}{\partial y}\right)^2+g\beta\sin\phi(T-T_\infty), \tag{2}$$

$$\rho c_p\left(u\frac{\partial T}{\partial x}+v\frac{\partial T}{\partial y}\right)=k\frac{\partial^2 T}{\partial y^2}-\frac{\partial q_r}{\partial y}+\Delta B_0^2 u^2\sin^2\psi$$
$$+\eta_0\left[1+\lambda^2\left(\frac{n-1}{2}\right)\left(\frac{\partial u}{\partial y}\right)^2+\lambda^4\frac{1}{2}\left(\frac{n-1}{2}\right)\left(\frac{n-3}{2}\right)\left(\frac{\partial u}{\partial y}\right)^4\right]\left(\frac{\partial u}{\partial y}\right)^2, \qquad (3)$$

where u and v are the x and y components of velocity respectively, η_0 the dynamic viscosity, Δ the electric conductivity, B_0 the uniform magnetic field strength, ρ the density of fluid, n the power index, λ the time constant, β the thermal expansion coefficient, c_p the specific heat at constant pressure, T the fluid, $T_s(x)$ the temperature interface, T_∞ the fluid temperature far from the surface, k the thermal conductivity of fluid, q_r the radiative heat flux, ψ the angle of magnetic field, ϕ the inclination angle of surface and ν the kinematic viscosity. The nonlinear form of thermal radiation is

$$q_r=-\frac{4\delta^*}{3k^*}\frac{\partial T^4}{\partial y}=-\frac{16\delta^*}{3k^*}T^3\frac{\partial T}{\partial y},$$
$$\frac{\partial q_r}{\partial y}=-\frac{16\delta^*}{k^*}T^2\left(\frac{\partial T}{\partial y}\right)^2-\frac{16\delta^*}{3k^*}T^3\frac{\partial^2 T}{\partial y^2}, \qquad (4)$$

in which δ^* is the Stefan-Boltzmann constant and k^* the mean absorption coefficient. The corresponding boundary conditions are

$$\eta_0\left[1+\lambda^2\left(\frac{n-1}{2}\right)\left(\frac{\partial u}{\partial y}\right)^2+\lambda^4\frac{1}{2}\left(\frac{n-1}{2}\right)\left(\frac{n-3}{2}\right)\left(\frac{\partial u}{\partial y}\right)^4\right]\left(\frac{\partial u}{\partial y}\right)=-\frac{d\delta}{dT}\frac{dT}{dx},$$
$$v(x,y)=v_w,\ T(x,y)=T_s=Ax^2+T_0, \qquad \text{at } y=0, \qquad (5)$$
$$u\to 0,\ T\to T_\infty=Bx^2+T_0, \qquad \text{when } y\to\infty, \qquad (6)$$

where v_w is constant mass transfer velocity with $v_w<0$ for suction and $v_w>0$ for injection, A and B the temperature gradient coefficients and δ the surface tension. Setting

$$\eta=c_1 y,\ \Psi(x,y)=\frac{x}{c_2}f(\eta),\ u=\frac{\partial\Psi}{\partial y},\ v=-\frac{\partial\Psi}{\partial x},$$
$$c_1=\sqrt[3]{\frac{\rho A(d\delta/dT)}{\mu^2}},\ c_2=\sqrt[3]{\frac{\rho^2}{\mu A(d\delta/dT)}},\ \theta=\frac{T-T_\infty}{T_s-T_0}, \qquad (7)$$

equation (1) is trivially verified whereas the dimensionless boundary layer problems are

$$f'^2-ff''=f'''\left[1+\frac{n-1}{2}\lambda_1 f''^2\right]+\lambda_1 f''' f''^2(n-1)\left[1+\frac{3}{4}\left(\frac{n-3}{2}\right)\lambda_1 f''^2\right]$$
$$+\beta^*\sin\phi\theta-M^2\sin^2\psi f', \qquad (8)$$

$$\theta''+4R(\theta_r-\theta_s)[1+(\theta_r-\theta_s)\theta]^2\theta'^2+\frac{4}{3}R[1+(\theta_r-\theta_s)\theta]^3\theta''$$
$$+\Pr E_c\left[1+\left(\frac{n-1}{2}\right)\lambda_1 f''^2+\frac{1}{2}\left(\frac{n-1}{2}\right)\left(\frac{n-3}{2}\right)\lambda_1^2 f''^4\right]f''^2 \qquad (9)$$
$$-\Pr[2S_t f'+2f'\theta'-f\theta']+M^2\Pr E_c\sin^2\psi f'^2=0,$$

$$\left[1+\left(\frac{n-1}{2}\right)\lambda_1 f''^2+\frac{1}{2}\left(\frac{n-1}{2}\right)\left(\frac{n-3}{2}\right)\lambda_1^2 f''^4\right]f''=-2, \quad (10)$$

$$f=\alpha,\ \theta=1-S_t,\ \text{at}\ \eta=0,$$
$$f'\to 0,\ \theta\to 0,\ \text{when}\ \eta\to\infty. \quad (11)$$

In above equations

$$\lambda_1=\frac{\lambda^2 c_1^4 x^2}{c_2^2},\ \beta^*=\frac{g\beta A x c_2^2}{c_1^2}, M^2=\frac{\Delta B_0^2 c_2}{\rho c_1},\ E_c=\frac{c_1^2}{A c_p c_2^2},\ R=\frac{4\delta^* T_\infty^3}{k^* k},$$
$$\Pr=\frac{\eta_0 c_p}{k},\ S_t=\frac{B}{A},\ \theta_r=\frac{T_s}{T_\infty},\ \theta_s=\frac{T_0}{T_\infty},\ \alpha=-c_2 v_w, \quad (12)$$

where $f(\eta)$ is the dimensionless velocity, $\theta(\eta)$ the dimensionless temperature, R the radiation parameter, $\Pr$ the Prandtl number, M the Hartmann number, λ_1 the fluid constant, E_c the Eckert number, θ_r, θ_s the temperature constants, β^* the mixed convection parameter, S_t the stratification parameter and α is the porosity constant. Local Nusselt number is

$$Nu=\frac{q_w x}{k(T_s-T_0)},$$
$$q_w=-\left(k\frac{\partial T}{\partial y}+\frac{16\delta^*}{3k^*}T^3\frac{\partial T}{\partial y}\right)_{y=0}. \quad (13)$$

Nonlinear Nusselt number (Nu) is

$$\mathrm{Re}_x^{-1/2} Nu=-\left\{1+\frac{4}{3}R(1+(\theta_r-\theta_s)\theta(0))^3\right\}\theta'(0),\ with \mathrm{Re}_x=c_1^2 x^2. \quad (14)$$

3. Numerical procedure

In this study, the nonlinear equations (8)-(9) with highly nonlinear boundary conditions (10) are successfully solved by implementing an efficient numerical scheme Runge-Kutta Fehlberg fourth fifth (RKF-45) order. Marangoni convection flow is discussed numerically. The effects of pertinent parameters are scrutinized for the dimensionless velocity, temperature and the rate of heat transfer. The step size and convergence criteria are chosen to be 0.001 and 10^{-6} respectively. Asymptotic boundary conditions in Eq. (10) are approximated by using a value of 10 as follows:

$$\eta_{\max}=10,\ f'(10)=\theta(10)=0. \quad (15)$$

This ensures that all numerical solutions approached the asymptotic values correctly.

4. Analysis

This section comprises analysis of numerical results for the velocity and temperature profiles of an electrically conducting Carreau fluid due to porous inclined surface. Effectiveness of involved physical parameters is discussed through graphs and tables for the nonlinear thermal radiative heat transfer, applied magnetic field, inclination of applied magnetic field, mixed convection, porosity of inclined surface, thermal stratification, power index of Carreau fluid, inclination of surface, heat dissipation, convection-conduction characteristics and momentum-thermal diffusivity. Figures $1-5$ describe the dimensionless velocity ($f'(\eta)$) situations for the changing aspects of physical properties through assigning the particular values to involved parameters. Figures $6-10$ give thermal behavior of current flow situations by dimensionless temperature distributions ($\theta(\eta)$) and Figure 11 defines the varying heat flux through Nusselt number (Nu) . Table 1 is presented to see the parametric effects on numerical values of Nusselt number (Nu). Table 2 is expanded to compare the numerical values of $-f''(0)$ with Hayat et al. [25] for different values of Hartmann number (M).

The involved physical parameters are the radiation parameter (R), fluid constant (λ_1), Hartmann number (M^2), inclination of applied magnetic field (ψ), mixed convection parameter (β^*), porosity of inclined surface (α), thermal stratification parameter (S_t), power index (n), inclination of surface (ϕ), Eckert number (E_c), temperature constants ($\theta_r,\ \theta_s$), Nusselt number (Nu) and Prandtl number (Pr).

Figure 1 is sketched for the behavior of dimensionless velocity $f'(\eta)$ when two important physical parameters the fluid constant (λ_1) and the Hartmann number (M^2) increase. Enhancement of both fluid constant (λ_1) and Hartmann number (M^2) decelerates the fluid velocity $f'(\eta)$. In this peculiar flow situation, the enhancement of fluid constant (λ_1) is directly proportional to Marangoni number (c_1). Direct increase in λ_1 uplifts the surface tension rate with high density that eventually decelerates the fluid velocity. The accelerating behavior of velocity $f'(\eta)$ for the expansion of mixed convection parameter (β^*) and power index (n) is detected in Figure 2. The response of power index (n) is recorded for its two values i.e., $n=1$ and $n=3$. Obviously for $n=3$, fluid velocity $f'(\eta)$ has higher value than $n=1$. Figure 3 reported the upshots of porosity parameter (α) and inclination of surface (ϕ) on fluid velocity $f'(\eta)$. One can note that for increasing α (from $\alpha=0.5$ to $\alpha=1.5$), the fluid velocity $f'(\eta)$ significantly reduced. This situation occurs owing to the larger suction rate at $\alpha=1.5$. An interesting observation for enhancement in fluid velocity $f'(\eta)$ is also observed in Figure 3 via making the surface more inclined through increasing ϕ. Large values of inclination of applied magnetic field (ψ) and thermal stratification parameter (S_t) decay the fluid velocity $f'(\eta)$(see Figure 4). The applied magnetic field has greater decelerating impact on velocity when applied at $\psi=0$ and this effect decreases for higher values of inclination angle ($for\ \ \psi=\pi/4$ and $\psi=\pi/2$). Similar behavior of velocity is noted for thermal stratification parameter (S_t) in this Figure. Figure 5 is displayed for impact of radiation parameter (R) and Eckert number (E_c) on fluid velocity $f'(\eta)$. The intense radiations (by changing R from 0 to 5) provides the high kinetic energy for fluid flow that in turns accelerates fluid motion (by increasing $f'(\eta)$). Eckert number (E_c) (which is the heat dissipation factor) also has an accelerating effect (see Figure 5). Impact of varying radiation parameter (R) and Hartmann number (M^2) on temperature profile $\theta(\eta)$ has been displayed in figure 6. Two cases of magnetic field impact on temperature are discussed for increasing radiation parameter. Solid line gives the heated radiation effects in the absence of magnetic field ($M=0$) and dashes depicts the same thermal fluid nature in the presence of magnetic field ($M=1$). Clearly temperature $\theta(\eta)$ is increased for later case. The heated nature of Eckert number (E_c) and power index (n) is explained through Figure 7. Figure 8 is presented to examine the influence of mixed convection parameter (β^*) and stratification parameter (S_t) on temperature distribution $\theta(\eta)$. This figure depicts that for larger β^* and thermal stratification (S_t), the fluid's temperature $\theta(\eta)$ decays. In Figure 9, the impact of inclination angle (ϕ) on temperature profile $\theta(\eta)$ is studied for two cases of fluid constant (λ_1). Here solid line describes viscous fluid case with $\lambda_1=0$ and dashes depict the Carreau liquid flow situations with $\lambda_1=1$. In both situations, temperature profile $\theta(\eta)$ decreased but the fluid is more heated in case of Carreau liquid when compared with viscous fluid situation. Significant impacts of two constants ($\theta_r,\ \theta_s$) on temperature $\theta(\eta)$ are given through Figure 10. Both the temperature constants ($\theta_r,\ \theta_s$) have tendency to cool down the fluid but the interface temperature constant θ_r rapidly lowers the temperature when compared to θ_s. Nusselt number is discussed in Figure 11 for radiation parameter (R), fluid cons $\tan$t (λ_1), Eckert number (E_c) and thermal stratification parameter (S_t). Figure $11(a)$ indicates that the fluid constant (λ_1) and radiation parameter (R) enhance the Nusselt number whereas Figure $11(b)$ shows that Eckert number (E_c) and thermal stratification (S_t) have reverse effects on Nusselt number (Nu). Numerical treatment Nusselt number (Nu) for current situation is given in Table 1. Numerical values of Nusselt number (Nu) reveal that larger values of Hartmann number (M^2) , inclination of surface (ϕ), inclination of magnetic field (ψ) and Eckert number (E_c), the Nusselt number decays. On the other hand the Nusselt number enhances for larger values of fluid constant (λ_1), porosity parameter (α), radiation parameter (R) and thermal stratification parameter (S_t). Comparison for the numerical values of -$f''(0)$ is given in Table 2. It is observed in this table that the present results matches exactly with the existing literature [25] for $0 \leq M < 1$ and matches upto 4^{th} decimal place for values $M \geq 1$.

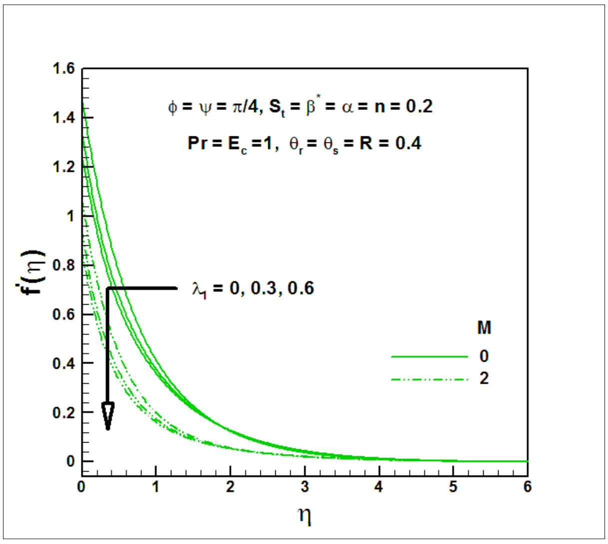

$Fig.1$: Effects of Hartmann number (M^2) and fluid constant (λ_1) on $f'(\eta)$.

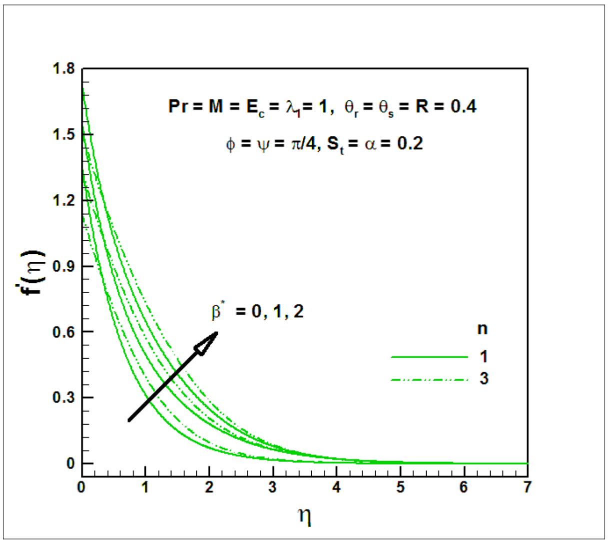

$Fig.2$: Effects of mixed convection parameter (β^*) and power index (n) on $f'(\eta)$.

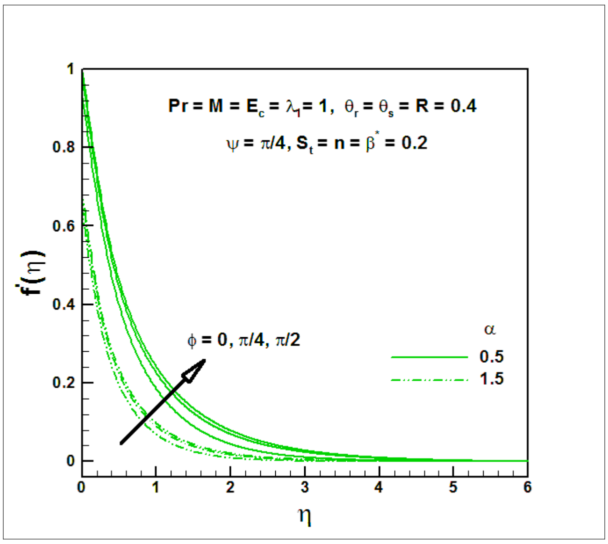

$Fig.3$: Effects of porosity constant (α) and surface inclination (ϕ) on $f'(\eta)$.

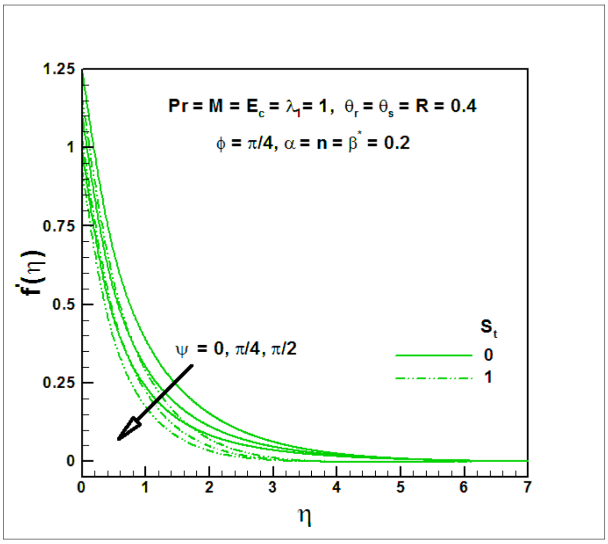

$Fig.4$: Effects of thermal stratification (S_t) and inclination of magnetic field (ψ) on $f'(\eta)$.

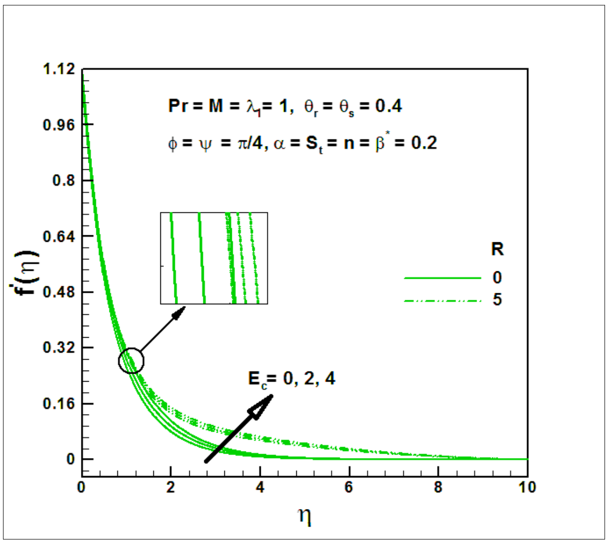

$Fig.5$: Effects of radiation parameter (R) and Eckert number (E_c) on $f'(\eta)$.

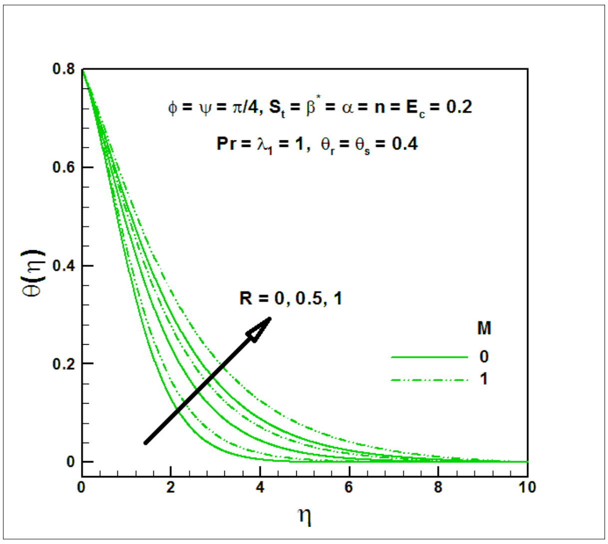

$Fig.6$: Effects of Hartmann number (M) and radiation parameter (R) on $\theta(\eta)$.

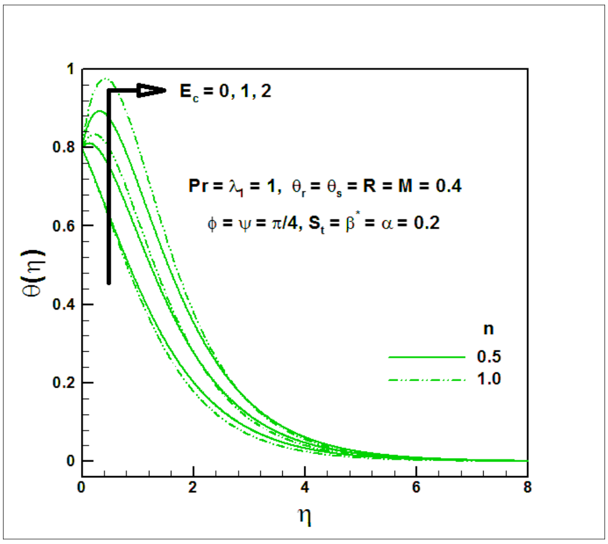

$Fig.7$: Effects of Eckert number (E_c) and power index (n) on $\theta(\eta)$.

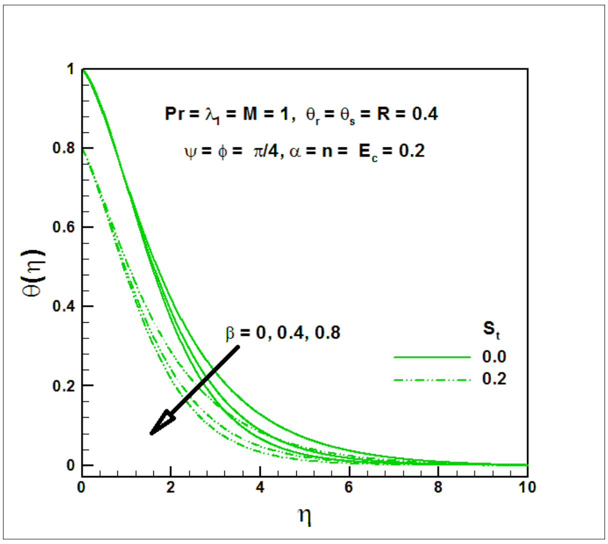

$Fig.8$: Effects of thermal stratification (S_t) and mixed convection (β^*) on $\theta(\eta)$.

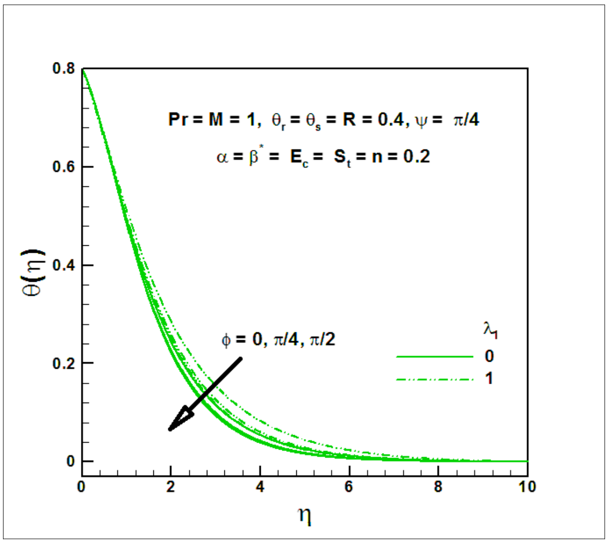

$Fig.9$: Effects of fluid constant (λ_1) and surface inclination (ϕ) on $\theta(\eta)$.

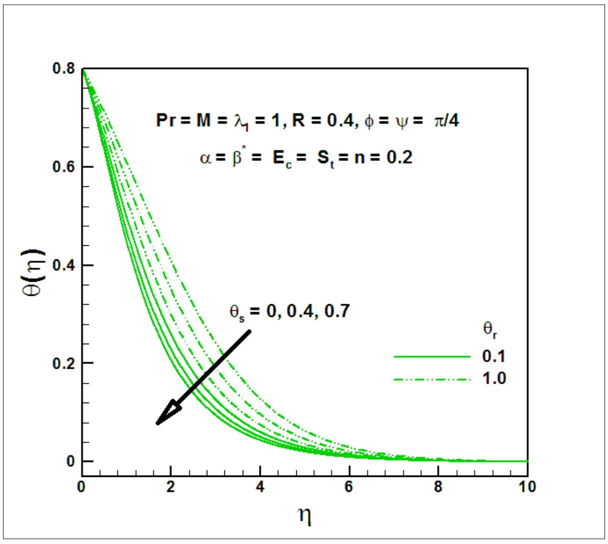

Fig.10 : Effects of interface temperature (θ_r) and reference temperature (θ_s) on $\theta(\eta)$.

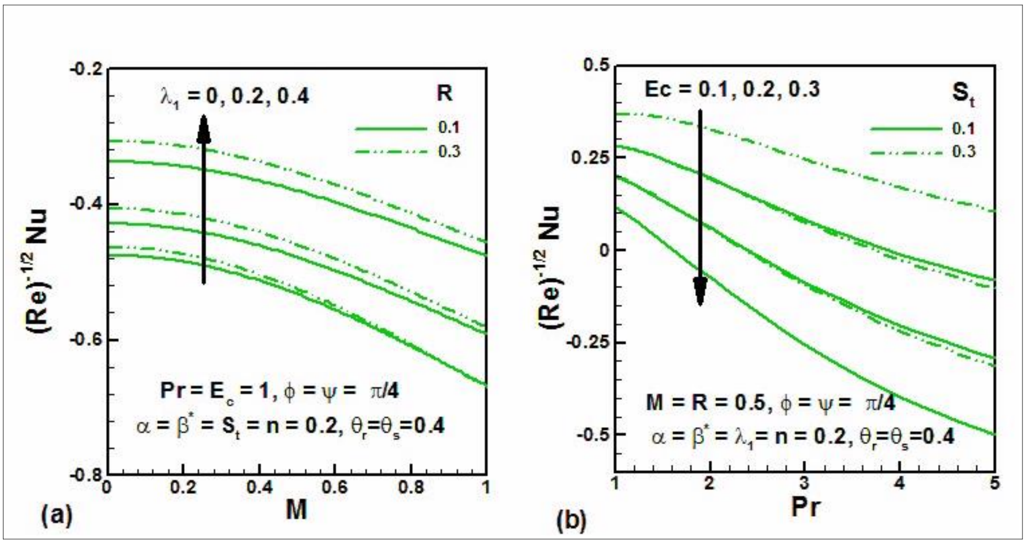

Fig.11 : Parametric effects on Nusselt number (N_u).

Table 1: Numerical values of Nusselt number for different physical parameters when $\Pr = 1$, $n = 0.2$, $\theta_r = 0.4$, $\theta_s = 0.3$ and $\beta^* = 0.2$.

M	λ_1	α	R	S_t	ϕ	ψ	E_c	$Re_x^{-1/2} Nu$
0	0.2	0.1	0.2	0.1	$\pi/3$	$\pi/4$	0.2	0.159728
0.2								0.158108
0.5								0.150117
1.0	0.1							0.142718
	0.3							0.172499
	0.5							0.186896
	0.2	0.2						0.191871
		0.3						0.228077
		0.4						0.268083
		0.1	0.0					0.085701
			0.5					0.260525
			1.0					0.404323
			0.2	0.0				0.069075
				0.3				0.328429
				0.5				0.483021
				0.1	$\pi/6$			0.159887
					$\pi/4$			0.159602
					$\pi/3$			0.159321
					$\pi/3$	$\pi/6$		0.159524
						$\pi/4$		0.159320
						$\pi/3$		0.159117
						$\pi/3$	0.0	0.332896
							0.1	0.245944

							0.3	0.072412

Table 2: Comparison of $-f''(0)$ with Hayat et al. [25] for different values of Hartmann number (M) when $\lambda_1=0$, n=1, $\alpha=0$, $\beta^*=0$, $\phi=0$, $\psi=90$.

M	$-f''(0)$	
	Hayat et al. [25]	RKF-45 (Present)
0.0	1.00000	1.00000
0.2	1.01980	1.01980
0.5	1.11803	1.11803
0.8	1.28063	1.28063
1.0	1.41421	1.41422
1.2	1.56205	1.56207
1.5	1.80303	1.80306

5. Conclusions

Numerical treatment is presented for the examination of Marangoni convective flow of magneto Carreau fluid over a permeable inclined surface with convective boundary conditions. The salient features are mentioned below.

- The inclination of surface and thermal stratification dampens the fluid motion and the heat transfer processes.
- Presence of Carreau fluid slows down the velocity but heats up the fluid.
- Nonlinear radiation behaves as regulating the fluid motion, Nusselt number and heat transfer processes.
- Fluid motion and heat transfer have reverse behavior for mixed convection parameter, Hartmann number and power index.
- Thermal field shows the opposite response for the reference and interface temperatures.

Acknowledgment: First author is grateful to the Higher Education Commission of Pakistan for the financial support through the National Research Project for Universities 2014 with Project No. 4090.

6. References

[1]. Zhao, J., *et al.*, Unsteady Marangoni convection heat transfer of fractional Maxwell fluid with Cattaneo heat flux, *Applied Mathematical Modelling*, *44* (2017), pp. 497-507.

[2]. Hayat, T., *et al.*, Impact of Marangoni convection in the flow of carbon--water nanofluid with thermal radiation, *International Journal of Heat and Mass Transfer, 106* (2017), pp. 810-815.

[3]. Sheikholeslami, M., Ganji, D. D., Influence of magnetic field on CuO-H2O nanofluid flow considering Marangoni boundary layer, *International Journal of Hydrogen Energy, 42* (2017), 5, pp. 2748-2755.

[4]. Aly, E. H., Ebaid, A., Exact analysis for the effect of heat transfer on MHD and radiation

Marangoni boundary layer nanofluid flow past a surface embedded in a porous medium, *Journal of Molecular Liquids, 215* (2016), pp. 625-639.

[5]. Hayat, T., *et al.,* Marangoni mixed convection flow with Joule heating and nonlinear radiation, *AIP Advances 5* (2015), 7, 077140.

[6]. Khan, M., *et al.,* On unsteady heat and mass transfer in Carreau nanofluid flow over expanding or contracting cylinder with convective surface conditions, *Journal of Molecular Liquids, 231* (2017), pp. 474-484.

[7]. Salahuddin, M., *et al.,* MHD squeezed flow of Carreau-Yasuda fluid over a sensor surface, *Alexandria Engineering Journal, 56* (2017), 1, pp. 27-34.

[8]. Hashim., Khan, M., On Cattaneo-Christov heat flux model for Carreau fluid flow over a slendering sheet, *Results in Physic, 7* (2017), pp. 310-319.

[9]. Abbasi, F. M., *et al.,* Numerical analysis for MHD peristaltic transport of Carreau-Yasuda fluid in a curved channel with Hall effects, *Journal of Magnetism and Magnetic Materials, 382* (2015), pp. 104-110.

[10]. Hayat, T., *et al.,* Hall and radial magnetic field effects on radiative peristaltic flow of Carreau-Yasuda fluid in a channel with convective heat and mass transfer, *Journal of Magnetism and Magnetic Materials, 412* (2016), pp. 207-216.

[11]. Hayat, T., *et al.*, Inclined magnetic field and heat source/sink aspects in flow of nanofluid with nonlinear thermal radiation, *International Journal of Heat and Mass Transfer*, *103* (2016), pp. 99-107.

[12]. Khan, A. U., *et al.,* Phase flow study of MHD nanofluid with slip effects on oscillatory oblique stagnation point flow in view of inclined magnetic field, *Journal of Molecular Liquids, 224* (2016), B, pp. 1210-1219.

[13]. Sivaraj, C., Sheremet, M. A., MHD natural convection in an inclined square porous cavity with a heat conducting solid block, *Journal of Magnetism and Magnetic Materials, 426* (2017), pp. 351-360.

[14]. Abbas, Z., *et al.,* Slip flow of magnetite-water nanomaterial in an inclined channel with thermal radiation, *International Journal of Mechanical Sciences, 122* (2017), pp. 288-296.

[15]. Shahzadi, I., Nadeem, S., Inclined magnetic field analysis for metallic nanoparticles submerged in blood with convective boundary condition, *Journal of Molecular Liquids, 230* (2017), pp. 61-73.

[16]. Bhatti, M. M., *et al.,* Mathematical modelling of nonlinear thermal radiation effects on EMHD peristaltic pumping of viscoelastic dusty fluid through a porous medium duct, *Engineering Science and Technology, an International Journal*, *20* (2017), 3, pp. 1129-1139.

[17]. Pal, D., Saha, P., Influence of nonlinear thermal radiation and variable viscosity on hydromagnetic heat and mass transfer in a thin liquid film over an unsteady stretching surface, *International Journal of Mechanical Sciences, 119* (2016), pp. 208-216.

[18]. Hsiao, K. L., Combined electrical MHD heat transfer thermal extrusion system using Maxwell fluid with radiative and viscous dissipation effects, *Applied Thermal Engineering, 112* (2017), pp. 1281-1288.

[19]. Cortell, R., MHD (magneto-hydrodynamic) flow and radiative nonlinear heat transfer of a viscoelastic fluid over a stretching sheet with heat generation/absorption, *Energy, 74*, (2014), 1, pp. 896-905.

[20]. Das, K., *et al.*, Radiative flow of MHD Jeffrey fluid past a stretching sheet with surface slip and melting heat transfer, *Alexandria Engineering Journal*, *54* (2015), 4, pp. 815-821.

[21]. Ali, H., Khan, M., Impact of heat transfer analysis on Carreau fluid flow past a static/moving wedge, *Thermal Science*, *22* (2018), 2, pp. 809-820.

[22]. Kairi, R. R., Free convection around a slender paraboloid of non-Newtonian fluid in a porous medium, *Thermal Science*, (2018) in press. https://doi.org/10.2298/TSCI170809005K

[23]. E. M. A. Elbashbeshy, *et al.*, Flow and heat ransfer over a stretching surface with variable thickness in a Maxwell fluid and porous medium with radiation, *Thermal Science*, (2018) in press. https://doi.org/10.2298/TSCI170228146E

[24]. Azimi, M., Riazi, R., Magnetohydrodynamic go-water nanofluid flow and heat transfer between two parallel moving disks, *Thermal Science*, *22* (2018), 1B, pp. 383-390.

[25]. Hayat, T., *et al.*, On model of Burgers fluid subject to magneto nanoparticles and convective conditions, *Journal of Molecular Liquids*, *222* (2016), pp. 181-187.